

# Structure and Penetration of a Supercritical Fluid Jet in Supersonic Flow

J. C. Hermanson,\* P. Papas,† and I. W. Kay‡

United Technologies Research Center, East Hartford, Connecticut 06108

The penetration characteristics and turbulent structure of transverse supercritical nitrogen (and reference subcooled liquid ethanol) jets were examined experimentally by the use of spark shadowgraph imaging. For given injection and freestream stagnation pressures, supercritical nitrogen jets penetrated significantly less into the supersonic stream than subcooled ethanol jets. The jet penetration further decreased with increases in the degree of superheat. The supercritical nitrogen jets were characterized by large-scale structure not generally observed for the case of subcooled ethanol injection. Practical difficulties inherent in the use of liquid fuel simulants in unheated supersonic flows for the simulation of supersonic combustion environments are discussed.

## Nomenclature

$C_d$	= discharge coefficient
$C_p$	= fluid specific heat
$D$	= jet diameter
$d_e$	= effective injector orifice diameter
$d_f$	= physical injector orifice diameter
$h$	= jet penetration height
$h_{fg}$	= latent heat of vaporization
$M$	= freestream Mach number
$P_a$	= freestream static pressure
$P_c$	= critical pressure
$P_v$	= fluid vapor pressure at injection temperature
$P_{0j}$	= jet stagnation pressure
$P_2$	= static pressure behind normal shock
$q$	= freestream dynamic pressure
$R$	= bubble radius
$T_B$	= boiling temperature at static pressure
$T_c$	= critical temperature
$T_i^*$	= dimensionless temperature parameter
$T_j$	= fluid injection temperature
$T_s$	= temperature of saturated liquid
$t_a$	= aerodynamic breakup time
$t_d$	= flash vaporization time
$t_{d1}$	= bubble induction time
$t_{d2}$	= bubble growth time
$u_a$	= freestream velocity
$u_j$	= jet injection velocity
$x$	= distance downstream of injector orifice
$\alpha$	= jet fluid thermal diffusivity
$\pi_i$	= dimensionless vapor pressure parameter
$P_a$	= freestream static density
$\rho_j$	= jet fluid density
$\sigma$	= surface tension

## Introduction

HERE is significant interest in the potential use of liquid, hydrocarbon fuels in propulsion systems for hypersonic

flight applications.<sup>1–4</sup> These fuels have high density, are storable, and are easily handled in comparison with cryogenic fuels. As such, they are attractive for future aircraft and missiles which may require the performance benefits offered by supersonic combustion ramjet (scramjet) propulsion systems. Consequent to these applications, there is significant interest in developing a means of promoting effective mixing and combustion of hydrocarbon fuels in supersonic combustors. One technique with the potential for achieving high levels of fuel dispersion exploits the violent disruption and flash-vaporization resulting from the injection of liquid at superheated or supercritical conditions. In practical applications, the hydrocarbon fuel would be used as a coolant to handle the high heat loads associated with hypersonic flight, and thus might subsequently be injected as superheated liquid.

The use of pressurized, preheated liquid hydrocarbon fuels in supersonic reacting flow was examined as part of a recent experimental study, in which high levels of combustor performance were achieved.<sup>4</sup> In those studies, much of the combustor testing was performed using Jet-A (JP-5), a liquid hydrocarbon, as the primary fuel; additional reference tests were conducted using gaseous ethylene fuel. During early tests in which the Jet-A was injected as an unheated liquid, very low combustion efficiencies were achieved. Subsequent injection of the Jet-A as a preheated liquid that flash-vaporized upon injection resulted in significantly higher combustion efficiencies. At low equivalence ratios, the efficiencies achieved with the preheated Jet-A were nearly identical to levels achieved with gaseous ethylene fuel. At higher equivalence ratios, it was suspected that poor penetration of the flash-vaporizing jet was the primary cause of the noticeably lower combustion efficiencies achieved with Jet-A vs those achieved with gaseous fuel.

The cost and difficulty of conducting experiments under actual scramjet combustor conditions provide a strong motivation for developing rational simulations using unheated supersonic flow. Numerous previous studies in unheated supersonic flow have examined the penetration, shock structure, and overall mixing characteristics of both sonic<sup>5–8</sup> and supersonic<sup>9–11</sup> transverse gas jets issuing into supersonic primary streams. There have also been studies of the structure, penetration, and atomization of liquid jets injected into supersonic streams<sup>12–14</sup> and flash-vaporizing liquid jets injected into stagnant gas.<sup>15–19</sup> Relatively little research has examined the case where the liquid is preheated or is in a supercritical state and flash-vaporizes upon injection into a supersonic crossflow.<sup>20–23</sup>

The experimental studies of the breakup of superheated liquid jets in a compressible crossflow that have been under-

Received Dec. 15, 1992; revision received Oct. 19, 1993; accepted for publication Oct. 20, 1993. Copyright © 1994 by United Technologies Corporation. Published by the American Institute of Aeronautics and Astronautics, Inc. with permission.

\*Research Scientist, Advanced Propulsion, Chemical Sciences, Senior Member AIAA.

†Graduate Research Associate; currently at the Department of Mechanical & Aerospace Engineering, Princeton University, Princeton, NJ 08540.

‡Senior Research Engineer, Advanced Propulsion, Chemical Sciences, Member AIAA.

taken are somewhat inconclusive as to the effect of flash-vaporization on jet penetration. For example, Newton and Dowdy<sup>20</sup> injected liquid nitrogen into supersonic streams of Mach numbers ranging from 2 to 4. In this case the flash-vaporization resulted in a decrease in jet penetration. Schetz et al.<sup>23</sup> studied the injection of Freon-12 into an unheated Mach 0.44 airstream and also noted a reduction in penetration height compared to room temperature water injection. Reichenbach and Horn,<sup>22</sup> however, noticed no change in penetration characteristics between jets of superheated acetone and those of room temperature water in tests conducted at similar flow conditions. These results point to a need for an improved fundamental understanding of the physics of liquid disruption, vaporization, and fuel/air mixing of liquid jets in compressible flows in order to provide design criteria for the successful development of supersonic combustion ramjet propulsion systems which may employ liquid hydrocarbon fuels.

Experiments utilizing an unheated supersonic flow dictate the use of a test liquid with a high vapor pressure at low temperatures if a rapid transition to vapor is to be achieved. For this reason, nitrogen, delivered above its critical pressure,  $P_c = 33.5$  atm, and near its critical temperature,  $T_c = 126$  K, was selected to serve as a fuel simulant in this work. The current study extends the earlier subcritical liquid nitrogen injection research by Newton and Dowdy<sup>20</sup> into the supercritical regime. Specifically, this work examines the effects of the flash-vaporization process on the structure and penetration characteristics of a thermodynamically unstable fluid jet in a supersonic crossflow.

### Theoretical Discussion

The process of the breakup of a liquid jet in a supersonic crossflow is rather complex, even in the absence of flash-vaporization. A simplified diagram of the principal features of the flowfield is shown in Fig. 1. The interaction of a transverse jet with a supersonic primary stream results in the former being swept downstream; the injected fluid serves in turn to obstruct the primary stream, giving rise to a bow shock upstream of the jet. Subsequent reflection of this shock wave from the flow channel walls can lead to additional pressure disturbances downstream of the injection site. In addition, the interaction of the bow shock with the boundary layer can give rise to a separation shock and a separation zone upstream of the injector site. The cohesive liquid core within this complicated, highly three-dimensional flowfield can develop wave structure on both the windward and leeward sides prior to the development of detached masses of liquid leading to eventual atomization.<sup>13</sup>

Joshi and Schetz<sup>14</sup> developed a correlation for the penetration of nonvaporizing jets over a wide range of freestream Mach numbers:

$$\frac{hM}{d_f} = 0.152 \left( \frac{\rho_j}{\rho_a} \right)^{0.5} \left( \frac{P_{o_j}}{P_a} \right)^{0.5} C_d \quad (1)$$

It should be noted that the correlation given by Eq. (1) is only valid in compressible flow, and in fact breaks down as the Mach number approaches zero. In addition to increasing with increasing pressure ratio  $P_{o_j}/P_a$ , the jet penetration also increases with increasing liquid/freestream gas density ratio  $\rho_j/\rho_a$ . Correlations based on other simple physical models are briefly surveyed by Kolpin et al.<sup>21</sup>; most of those models indicate similar dependencies on pressure and density ratios as does the correlation given in Eq. (1).

Some insight into the nature of the breakup of superheated liquid jets has been gained from experiments involving liquid injection into stagnant gas.<sup>15-19</sup> Lienhard and Day<sup>16</sup> proposed that the breakup of a liquid jet undergoing flash-vaporization in a stagnant environment be characterized by two characteristic times: an "idle" or "dwell" time for bubble nucleation

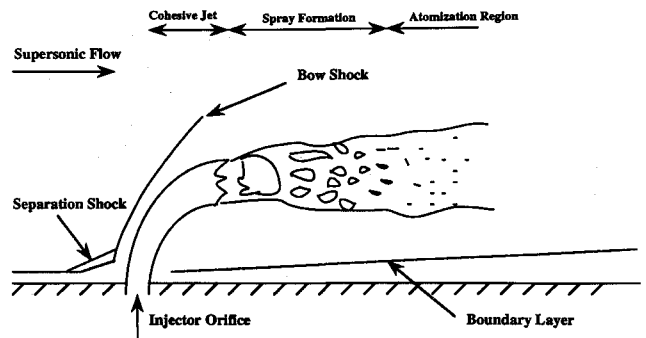


Fig. 1 Liquid jet in supersonic crossflow (adapted from Ref. 12).

inside the thermodynamically unstable liquid, followed by a growth time of these bubbles to sizes that will fracture the jet. An expression for a characteristic mean dwell time

$$\bar{t}_{d1} \sim \frac{\sigma^3 \sqrt{\rho_j}}{D^2 (P_v - P_a)^{7/2}} \quad (2)$$

was derived from dimensional arguments. A similar expression was derived by taking into consideration homogeneous nucleation, the force balance on a bubble, and the probability of nucleus survival until the onset of rapid bubble growth.<sup>15,16</sup> Equation (2) illustrates the strong impact that the degree of superheat (i.e.,  $P_v - P_a$ ) has on the dwell time.

The asymptotic growth time is in part controlled by the transfer of energy to the liquid-vapor interface of the bubbles and can be expressed as<sup>16</sup>

$$t_{d2} \approx \frac{D^2}{\pi \alpha} \left( \frac{h_{fg}}{c_p \Delta T} \right)^2 \left( \frac{\rho_a}{\rho_j} \right)^2 \quad (3)$$

where  $\Delta T \equiv T_j - T_s$  is the degree of superheat, i.e., the difference between the injectant fluid temperature and the saturation temperature.

The presence of a crossflow dictates that the breakup of a liquid jet also be characterized by an aerodynamic time scale. The aerodynamic breakup time can be represented as the penetration height divided by the liquid jet velocity. Reichenbach and Horn<sup>22</sup> expressed the jet velocity in terms of the injection pressure ratio to yield the following relationship for the aerodynamic breakup time<sup>22</sup>:

$$t_a \approx 4.8 (d_e \rho_j^{1/2} / M P_a^{1/2}) \quad (4)$$

where the effective injector orifice diameter  $d_e$  includes a correction for discharge coefficient. As long as  $t_a$  is less than the flashing time  $t_d \equiv t_{d1} + t_{d2}$ , the penetration should not be greatly impacted by flash-vaporization, and as such will obey the correlation given in Eq. (1).

Reichenbach and Horn<sup>22</sup> calculated characteristic times for their experiments and also for those of Newton and Dowdy<sup>20</sup>; in both cases the very short calculated asymptotic growth times  $t_{d2}$  suggest that the flashing process was governed by the nucleation time,  $t_{d1}$ . Reichenbach and Horn further concluded that in their experiment the aerodynamic breakup time  $t_a$  was shorter than the flashing time  $t_d$ . This conclusion stemmed from a lack of observable change in penetration with increasing superheat. Regarding the experiments of Newton and Dowdy, however, Reichenbach and Horn concluded that premature nucleation caused the nucleation stage to be completed while the liquid nitrogen was still in the injector, so that the overall breakup process was essentially due to flashing, rather than aerodynamic breakup. Characteristic calculations for the current experiment, based on the flash-vaporization data of Wu et al.,<sup>17</sup> suggest that at lower injection temperatures the flash-vaporizing times are comparable with the aerodynamic times; at higher liquid temperatures (and

hence, higher vapor pressures) the flashing time becomes an order of magnitude shorter than the corresponding aerodynamic times.

To account for the effects of flash-vaporization on jet penetration, Kolpin et al.<sup>21</sup> employed an empirical correction to the correlation given in Eq. (1), to get

$$\frac{hM}{d_c} = 6.77 \left[ \frac{P_{0j}}{P_a} \left( \frac{P_2}{P_v} \right)^n \right]^{0.51} \quad (5)$$

The empirically determined values of the exponent were  $n = 0.25$  for  $P_v > P_2$ , and  $n = 0$  for  $P_v < P_2$ ; the latter value corresponding to the case without flash-vaporization.

The penetration heights of Newton and Dowdy,<sup>20</sup> when correlated with Eq. (5), compared well with the room temperature water results of Reichenbach and Horn.<sup>22</sup> Reichenbach and Horn also studied the effect of vapor pressure on the penetration of superheated acetone and water jets in supersonic flow. The correction based on vapor pressure was evidently not required for the superheated acetone and water jets. Issues pertaining to this comparison are discussed later in this article.

### Experimental Investigation

Nitrogen at supercritical pressure and subcooled (i.e., below saturation temperature) liquid ethanol were employed as injectant fluids in these experiments. It was desired to simulate the structure and penetration characteristics of a liquid, hydrocarbon fuel stream undergoing flash-vaporization in a scramjet device where the supersonic flow would be at a higher static temperature than that of the fuel. The relatively low static temperature (170 K at Mach 2) of the unheated supersonic flow in this experiment dictated the use of a fuel simulant with high vapor pressure at low temperature to ensure flash-vaporization at test section conditions. This consideration, as well as those of availability and environmental impact, led to the selection of nitrogen as an injectant fluid. Unheated ethanol liquid was chosen to serve as a baseline, nonflash-vaporizing liquid for comparison with the flash-vaporizing supercritical nitrogen. The relatively low freezing point of ethanol (156 K) precluded freezing at the low primary stream static temperatures of this investigation.

### Apparatus

Experiments were performed in a small-scale supersonic flow facility. This facility was described in detail in a previous paper<sup>8</sup> and is only briefly described here; a schematic diagram of the facility is shown in Fig. 2. Dry nitrogen gas from compressed gas cylinders was supplied to a settling chamber 51 mm in diam and 64 mm in length. The stagnation pressure and temperature of the primary flow were measured, respectively, by a static pressure probe situated in the settling chamber and by a thermocouple in the nitrogen supply line. The contraction and nozzle section was 135 mm in length. Nozzle blocks were installed to produce a nominal test section Mach number of 2.0 for this experiment.

The test section employed in this study was  $12.7 \times 12.7$  mm in cross section and 140 mm in length. The test section consisted of top and bottom walls fashioned from aluminum, with optical access provided from sidewalls fabricated from quartz plate. The flush injector orifice (0.30-mm diam) was situated in the bottom wall 50 mm downstream from the beginning of the test section. The walls of the injector orifice plenum consisted of a 45-deg half-angle cone joined at its apex to a straight section 1.3 mm in length. Calibration with pressurized water indicated a discharge coefficient of approximately  $C_d = 0.75$ . The temperature of the injectant fluid was measured using a type-T (copper-copper/nickel) thermocouple mounted in the supply line immediately upstream of the injector orifice. A wall static pressure tap was situated 28 mm upstream of the injector orifice, on the opposite wall.

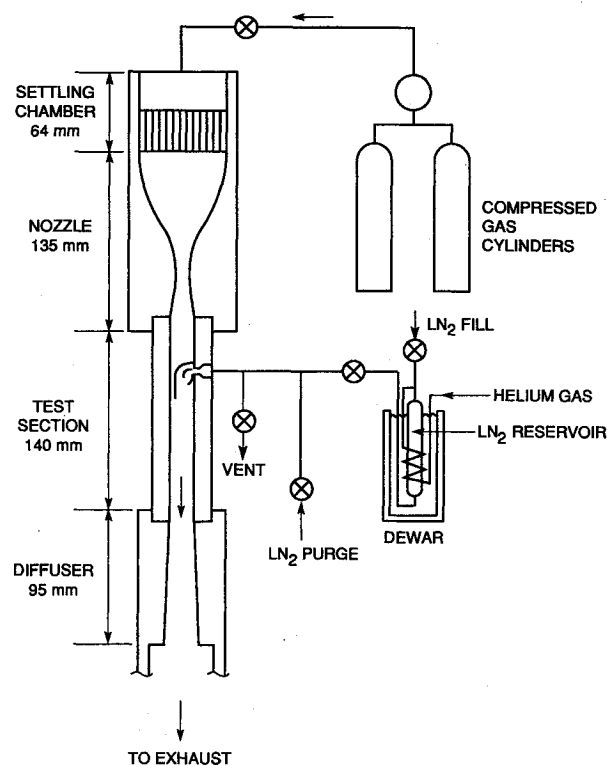


Fig. 2 Schematic of flow facility.

Downstream of the test section, pressure recovery was accomplished by a diffuser section 80 mm in length connected to an exhaust blower located outside the laboratory.

The injectant fluids were contained prior to each run in a pressurized flask of 300-ml volume. This volume allowed for a fluid injection time of roughly 30 s at a representative supply pressure of 40 atm. For the case of nitrogen injection, the flask was submerged in a liquid-nitrogen bath. The flask was held at constant pressure during fluid discharge by means of pressurized helium gas that was precooled to the saturation temperature of the liquid nitrogen (77 K @ 1 atm) via a cooling coil immersed in the liquid-nitrogen bath (see Fig. 2). Helium was chosen as the pressurizing agent because it remains gaseous under the injection conditions of this experiment. The pressure in the flask was measured with a cryogenic pressure transducer. The supply line connecting the flask to the injection orifice was cooled prior to the beginning of each experiment by purging with liquid nitrogen from a separate dewar.

Flow visualization was accomplished by spark shadowgraph imaging. Illumination was provided by an air gap spark of roughly  $0.3\text{-}\mu\text{s}$  duration. An  $f/10$  parabolic mirror collimated the spark source into a parallel beam which transited the test section parallel to the injector wall. The shadowgraph image was then captured directly at the focal plane of a 35-mm camera mounted approximately 100 mm from the test section centerline.

### Flow Conditions

The supersonic freestream was at a nominal Mach number of  $M = 2.0$  at stagnation pressures and temperatures ranging respectively from 3.0 to 3.7 atm, and 279 to 283 K. Wall static pressure measurements for the case without injection (i.e., primary flow only) indicated a Mach number at the test section entrance of  $M = 1.84$ . The corresponding static pressure and temperature conditions ranged from 0.49 to 0.61 atm and 166 to 169 K, respectively. The injectant stagnation pressure ranged from 34 to 57 atm for the supercritical nitrogen experiments, and from 17 to 54 atm for the liquid ethanol experiments. The temperature of the nitrogen at the injection orifice varied from roughly 113 to 125 K; ethanol was injected at room

temperature ( $\approx 293$  K). The turbulent boundary-layer thickness at the injector site was estimated visually from shadowgraph images to be roughly 1.1 mm. The Mach number decreased roughly 6% over the length of the test section due to boundary-layer growth.<sup>8</sup>

### Experimental Results

Spark shadowgraph images of the flowfield for the case of supercritical nitrogen injection are presented in Figs. 3 and 4a–4b. The three images shown in Fig. 3 are all at the same flow conditions and serve to illustrate typical shot-to-shot variations in turbulent structure. Representative images for two other flow conditions are shown in Figs. 4a and 4b. The flow is from left to right with the injector wall at the bottom of each image. The location of the injector orifice is shown in each figure. Locations corresponding to downstream distances normalized by the effective orifice diameter of  $x/d_e = 30$ , and  $x/d_e = 60$ , where  $x$  is the distance downstream of the injection site, are also shown for reference. The large density difference between the injectant fluid and the supersonic primary gas is

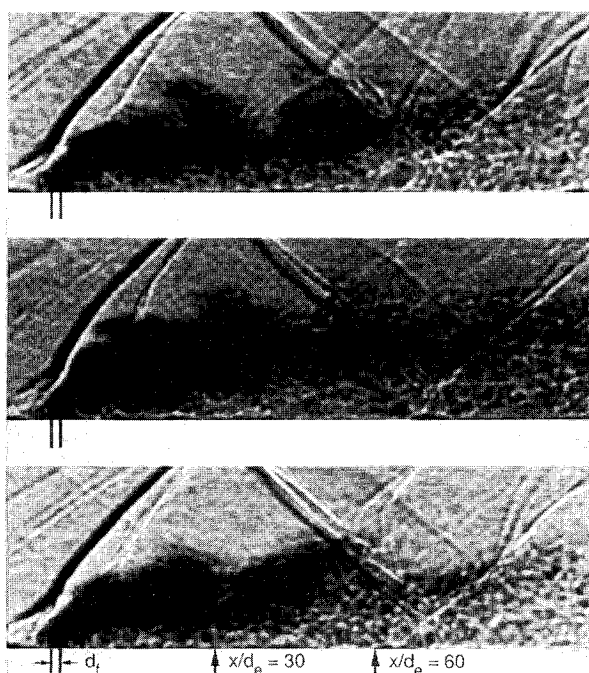


Fig. 3 Spark shadowgraph images of nitrogen jet injected at supercritical pressure into  $M = 1.84$  supersonic flow. All images are at the same flow conditions:  $P_{o_z} = 4.1$  atm,  $P_{o_j} = 58.1$  atm,  $T_{o_j} = 114$  K.

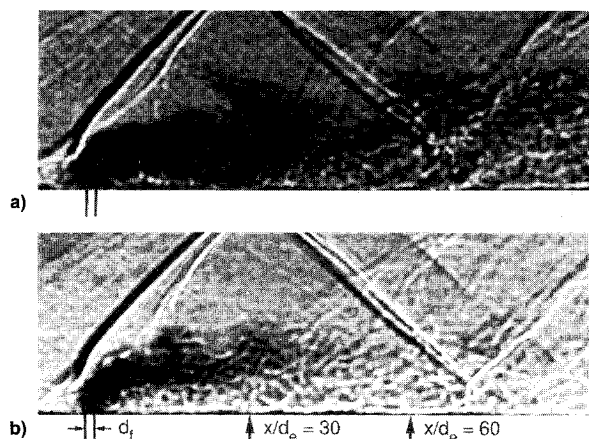


Fig. 4 Spark shadowgraph images of nitrogen jet injected at supercritical pressure into  $M = 1.84$  supersonic flow: a)  $P_{o_z} = 3.0$  atm,  $P_{o_j} = 35.2$  atm,  $T_{o_j} = 115$  K and b)  $P_{o_z} = 3.4$  atm,  $P_{o_j} = 48.6$  atm,  $T_{o_j} = 125$  K.

conductive to good shadowgraph visualization of the flow structure. For the nitrogen injection experiments shown in Figs. 3 and 4, large structures are observable for normalized distances that range from  $15 < x/d_e < 55$ , and are typically well developed by  $x/d_e \approx 30$ .

Structural features continue to be visible well downstream of the injection site, persisting until the transition from fluid to vapor is complete at  $35 < x/d_e < 60$ . Downstream of this point large-scale structural features are not visible using the current visualization technique, although the boundary of injectant fluid can still be discerned. The jet does not appear to achieve its maximum penetration until a normalized downstream distance of roughly  $x/d_e \approx 30$ . This distance is somewhat greater than for the case of gas-phase jets,<sup>8,9</sup> where the maximum penetration height is essentially attained by  $x/d_e \approx 10$ . The shadowgraph images also suggest that regions of unmixed primary stream gas penetrate well into the profile of the transverse fluid jet, consistent with observations of gas-phase jets in compressible flow.<sup>8</sup> It should be noted that at least part of the regions in question may consist of vaporized injectant fluid rather than primary stream gas. The sense of rotation of the large structures seen in Figs. 3 and 4 cannot be determined from the current results, as shadowgraph imaging is line-of-sight, and, in addition, only single-shot images were acquired.

Spark shadowgraph images of subcooled liquid-ethanol jets are shown in Figs. 5a and 5b. The low static temperature of the supersonic primary stream precluded any significant vaporization of this fluid. The liquid-gas interface is clearly visible, but large-scale structure is generally not as apparent as in the case of supercritical nitrogen injection. The horizontal streaks visible in some of the images in Fig. 5 are the tracks of ethanol droplets deposited on the wall from a previous run. The maximum penetration of these subcooled liquid jets appears to be achieved at roughly the same range of downstream location as for supercritical fluid jets, i.e.,  $x/d_e \approx 30$ .

The nitrogen fluid jet at supercritical injection conditions exhibits a lower penetration at a given downstream distance than a subcooled ethanol liquid jet injected at an identical pressure ratio  $P_{o_j}/P_a$ . A similar value of  $P_{o_j}/P_a$  also implies, assuming constant discharge coefficient, a comparable jet/freestream momentum flux ratio  $J \equiv (\rho_j u_j^2 / \rho_\infty u_\infty^2)$ . The observed penetration heights, scaled by Mach number and effective orifice diameter, are plotted in Fig. 6 vs the measured pressure ratio. The trend towards decreased jet penetration with increasing superheat is in qualitative agreement with earlier results,<sup>20,23</sup> in which superheated liquids injected at subcritical pressure exhibited lower penetration than nonsuperheated liquid jets. Penetration heights were measured from

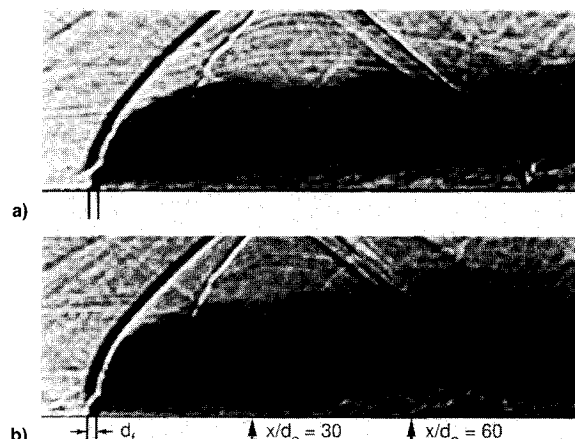


Fig. 5 Spark shadowgraph images of subcooled ethanol jet injected at supercritical pressure into  $M = 1.84$  supersonic flow: a)  $P_{o_z} = 3.4$  atm,  $P_{o_j} = 33.3$  atm,  $T_{o_j} = 293$  K and b)  $P_{o_z} = 3.4$  atm,  $P_{o_j} = 39.4$  atm,  $T_{o_j} = 293$  K.

the shadowgraph images at a normalized downstream distance of  $x/d_e = 100$ . The scaling law<sup>21</sup>  $h/d_e \sim (x/d_e)^{0.4}$  was employed to rescale the results presented by Reichenbach and Horn<sup>22</sup> and Kolpin et al.<sup>21</sup> from  $x/d_e = 150$  to  $x/d_e = 100$  to facilitate comparison with the current results.

The room temperature ethanol jet penetrations of the current work are seen in Fig. 6 to be in reasonable agreement with the room temperature water and acetone results of previous investigators.<sup>22</sup> Since the ratio of vapor pressure to static pressure at the injection site is quite small for the room-temperature acetone, ethanol, and water experiments, one would expect the penetration characteristics of these thermodynamically stable jets to be similar. As the degree of superheat of the injected fluid increases (i.e.,  $P_2/P_v$  decreases), however, the normal penetration of the jet might be expected to diminish as the transition to vapor and the breakup of the jet becomes more rapid. This is confirmed by the current results, where nitrogen jets with vapor pressure ratios of  $P_2/P_v \approx 0.1$  do penetrate less into the supersonic flow than the unheated liquid jets; the cases for which  $P_2/P_v \approx 0.05$  penetrate still less. The nitrogen injection data of Newton and Dowdy<sup>20</sup> which are characteristic of a ratio of static pressure to vapor pressure of about  $P_2/P_v \approx 0.1$  also show the expected reduced normal penetration relative to room temperature liquid, in agreement with the current work.

The observed penetration heights in the current work at  $x/d_e = 30$ , scaled by Mach number and effective orifice diameter, are presented in Fig. 7. Penetration heights were estimated by fairing a smooth, monotonically increasing curve through the edges of structural features farthest from the wall and recording the height of each such curve at  $x/d_e = 30$ . Especially for the case of supercritical nitrogen injection, the

liquid-vapor interface is somewhat more distinct at  $x/d_e = 30$  than at  $x/d_e = 100$ , owing to the presence of large amounts of nonvaporized fluid. The somewhat larger variations in measured penetration height for nitrogen injection than for the case of liquid ethanol injection are due both to the large structures at  $x/d_e = 30$  as well as to variations in superheat level within each data set identified in Fig. 7. The trend of decreasing jet penetration with increasing superheat remains, however, in qualitative agreement with the results presented in Fig. 6.

It should be noted that the penetration measurements cited for  $x/d_e = 100$  are downstream of the intersection of the first reflected shock with the transverse jet. Although the reflected shocks visible in the figures are of finite strength, there does not appear to be any systematic effect of the shock/jet interaction on the jet penetration, as determined visually from the figures. This conclusion is supported by the qualitative agreement between the penetration results for  $x/d_e = 30$ , which is well upstream of the reflected shock/jet intersection, and those for  $x/d_e = 100$ .

### Discussion

The mechanisms which give rise to the observed large-scale structure are not entirely clear. Kush and Schetz<sup>13</sup> state that aerodynamically induced waves are a dominant mechanism leading to jet breakup, and observed such waves in nonvaporizing liquid jets. It is unclear whether these waves arise solely from the primary stream/jet interaction, or whether they might be a consequence of oscillations in the position of the bow shock.<sup>24</sup> It is also unclear why the large-scale structure becomes more apparent with increasing superheat. One possibility is an unsteadiness in the jet injection due to flash-vaporization. For example, Newton and Dowdy<sup>20</sup> acknowledge the possibility of premature boiling in the jet plenum prior to injection. This phenomenon is, however, less likely in the current experiment due to the supercritical pressures at which the fluid is injected. Interfacial instability can also be driven by rapid vaporization,<sup>25</sup> although calculations based on the jet size and injectant flow rate indicate that the interfacial mass flux due to flash-vaporization in the current study is roughly two orders of magnitude smaller than that required to drive this type of instability mechanism.

It can be noted from Fig. 6 that some of the Newton and Dowdy<sup>20</sup> liquid nitrogen penetration data agree with those of the room temperature water correlation. The ratio of static pressure to vapor pressure  $P_2/P_v$  at the injection site, however, is about unity for this subset of the Newton and Dowdy experiments. The superheated acetone and water results of Reichenbach and Horn also do not exhibit a decrease in penetration as compared with unheated liquid injection results. Reichenbach and Horn attributed this to the aerodynamic time being much shorter than the nucleation time in the experiments considered.

An alternate explanation of this discrepancy can be derived from consideration of the vapor pressures of the test fluids utilized. The vapor pressures are plotted in Fig. 8 vs temperature. The rectangular regions in the figure denote the range of freestream static pressures of the works of Reichenbach and Horn,<sup>22</sup> Newton and Dowdy,<sup>20</sup> and the current study. Liquids such as acetone, ethanol, and water have relatively low vapor pressure at room temperature, as shown in the figure. In order to obtain a vapor-pressure to static-pressure ratio comparable to that of Newton and Dowdy,<sup>20</sup> Reichenbach and Horn<sup>22</sup> heated acetone and water to temperatures exceeding 400 K. In contrast to both Newton and Dowdy's experiment and the supercritical injection cases of the current work, the injectant fluids in Reichenbach and Horn's experiments were characterized by lower vapor pressures at the static temperature of the freestream than at injection. This implies that the vapor pressures of their injectants tended to continually decrease with downstream distance as the injectant fluid was cooled by the cold supersonic stream. The at-

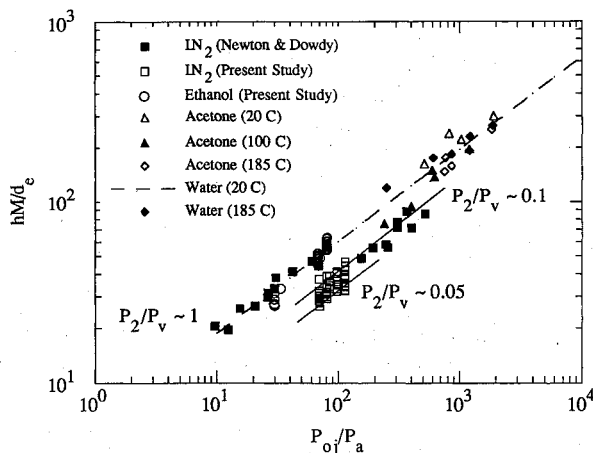


Fig. 6 Normalized jet penetration comparison at  $x/d_e = 100$ . The values of the pressure ratio  $P_2/P_v$  are for nitrogen injection only.

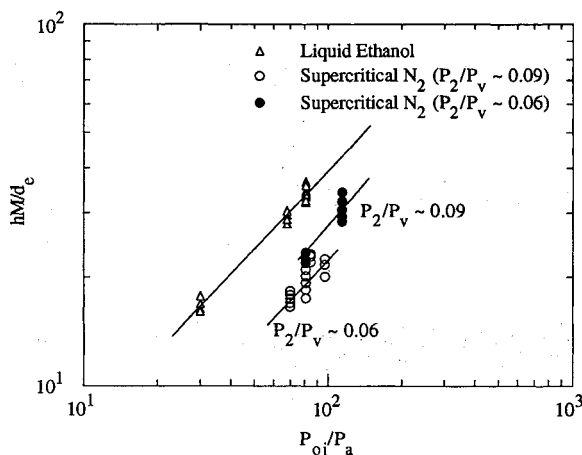


Fig. 7 Normalized jet penetration comparison at  $x/d_e = 30$ .

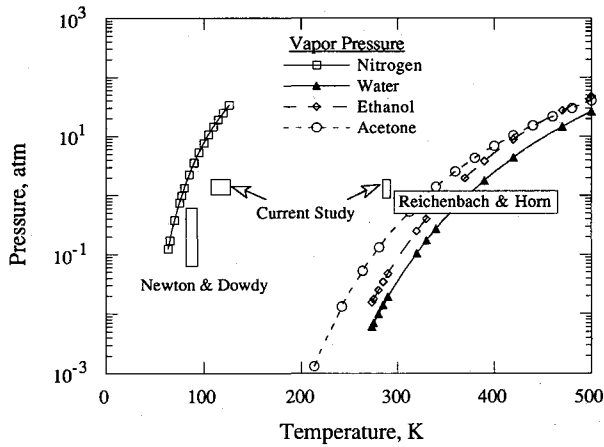


Fig. 8 Comparison of test conditions. Rectangles, freestream static pressures and fluid injection temperatures; curves, vapor pressure.

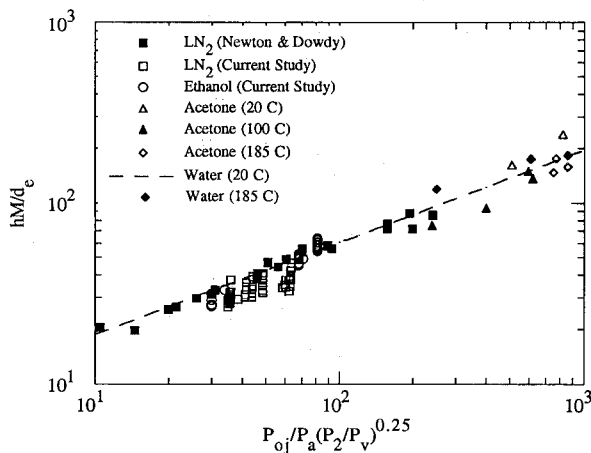


Fig. 9 Normalized jet penetration and vapor pressure correlation of Kolpin et al.<sup>21</sup>

tendant reduction in vaporization rate may partially explain why the superheated jets did not exhibit a noticeable decrease in penetration compared with jets injected at room temperature. Although much of the vaporization occurs near the injection site, the shadowgraphs of supercritical nitrogen jets do suggest that some unvaporized fluid remains well downstream (possibly as far as to  $35 < x/d_e < 60$ ). It is probably in this downstream region that the vaporization rate would be most affected by flow cooling, with a commensurate impact on mixing and penetration.

The validity of the empirical correlation developed by Kolpin et al.<sup>21</sup> [Eq. (5)] to account for the effects of flash-vaporization on jet penetration was examined by plotting the current penetration results as a function of the parameter  $(P_{oj}/P_a)(P_2/P_v)^{0.25}$ , as shown in Fig. 9. The choice of the pressure ratio  $P_2/P_v$  as a correlating parameter is physically reasonable, in that the degree of flash-vaporization depends most strongly on the enthalpy, which is a strong function of temperature (and hence, vapor pressure  $P_v$ ), but only weakly dependent on pressure for fluids at or below the critical temperature.

The correlation [Eq. (5)] appears to be only effective for those data in the current investigation with a comparable degree of superheat (i.e.,  $P_2/P_v$ ) to those of Newton and Dowdy.<sup>20</sup> That agreement might be expected, as the correlation was in fact derived from the data of Newton and Dowdy. The higher degrees of superheat (i.e., smaller values of  $P_2/P_v$ ) in the current work appear to be outside the useful range of the correlation. This suggests that this correlation may not capture the essential physics of vaporization and jet penetration for the case of supercritical injection. For example, the

maximum fraction of liquid that will theoretically flash-vaporize in an isenthalpic expansion ranged from roughly 40–70% in the current work. This substantially exceeded the 9–15% flash-vaporization attained in the work of Newton and Dowdy.

The comparison between Newton and Dowdy's experiment<sup>20</sup> and that of Reichenbach and Horn<sup>22</sup> indicates, as discussed above, that the amount of jet penetration into a supersonic crossflow depends not only on the initial degree of jet superheat, but is also impacted by the variation in vapor pressure associated with temperature changes due to heat transfer between the injectant fluid and the supersonic stream. For example, in the scramjet combustion investigation of Kay et al.,<sup>4</sup> fuel was injected at a temperature of about 600 K compared with a static temperature of up to 1400 K behind the bow shock. This temperature difference between injectant and primary stream was thus of reverse sign than the experiments of Reichenbach and Horn,<sup>22</sup> where liquids were injected at temperatures of 300–560 K into a supersonic flow with maximum static temperatures of 300 K. Thus, while the experiment of Reichenbach and Horn could have achieved a comparable initial degree of superheat to the combustor tests of Kay et al., the vapor pressure of the injectant would have changed in a fundamentally different manner with downstream distance, possibly impacting the penetration characteristics of the jet. This could have important implications in designing experiments to simulate the fuel dispersion and fuel/air mixing characteristics of a scramjet combustor by using fuel simulants in unheated supersonic flow. Acceptable simulations therefore require consideration of both the degree of superheat and the actual temperature difference between the supersonic flow and the injectant. Other factors would include injector configuration and flow rate, Mach number, liquid density, viscosity, and surface tension.<sup>23</sup>

The adequacy of a simulation can be quantified by use of the following nondimensional parameters<sup>23</sup>:

$$\pi_i(T) \equiv \frac{P_v - P_a}{q_\infty}$$

$$T_i^* \equiv \frac{T_{0_\infty} - T_j}{T_{ref}}$$

where  $T_{ref}$  is a reference temperature. Schetz et al.<sup>23</sup> suggested that a reasonable choice of reference temperature is  $T_{ref} \equiv T_B - T_j$ , where  $T_B$  is the boiling temperature of the injectant fluid at the ambient static pressure. Using this definition and expressing the freestream dynamic pressure as  $q_\infty = (\gamma/2)P_a M^2$  allows rewriting the above two parameters as

$$\pi_i(T) = \frac{2}{\gamma M^2} \left[ \frac{P_v}{P_a} - 1 \right]$$

$$T_i^* = \frac{T_{0_\infty} - T_j}{T_B - T_j}$$

Values of these parameters are presented in Table 1 for the current investigation and previous studies discussed in this article. The range of the temperature parameter in the current study was comparable to that of the scramjet investigation of Kay et al.,<sup>4</sup> although the current results are at somewhat higher normalized vapor pressures. The work of Newton and Dowdy<sup>20</sup> was performed over a similar range of the pressure parameter  $\pi_i$ , but with somewhat different values of the temperature parameter  $T_i^*$ . This is a consequence of both the lower jet injection temperatures as well as lower freestream static pressures in their work as compared with the current study. The values of superheat parameters for the experiments of Schetz et al.<sup>23</sup> were chosen to simulate ramjet, rather than scramjet, conditions.

Table 1 Values of superheat parameters

Investigation	Injectant	Primary stream	$\pi_i$	$T_i^*$
Current study	Nitrogen at supercritical pressure	$M = 1.84$ unheated nitrogen	+11.5 to +27.0	-4.2 to -2.9
Kay et al. <sup>4</sup>	Jet-A	$M = 3.0$ heated air	+7.1 to +8.0	-5.4 to -3.9
Newton and Dowdy <sup>20</sup>	Liquid nitrogen at subcritical pressure	$M = 2.01$ to $M = 3.99$ slightly heated air	+4.2 to +21.0	-13.8 to -6.7
Schetz et al. <sup>23</sup>	Freon-12	$M = 0.44$ unheated air	-6.3 to -0.62	-0.5 to +2.5
Reichenbach and Horn <sup>22</sup>	Superheated water	$M = 2.8$ and $M = 4.0$ unheated air	+0.10 to +18.1	+1.1 to +6.4
Reichenbach and Horn <sup>22</sup>	Superheated acetone	$M = 2.8$ and $M = 4.0$ unheated air	+0.97 to +35.7	+0.76 to +1.1

In any case, a clear contrast exists between the experimental conditions of Reichenbach and Horn<sup>22</sup> and both the actual scramjet conditions as well as the nitrogen injection simulations. This is clearly illustrated by the change in sign of the temperature parameter  $T_i^*$ . This sign change reflects the difference discussed above between the vaporization characteristics of a jet which is heated by the surrounding gas vs those of a jet subject to cooling.

The reasonable agreement in the values of superheat parameters between the current cold-flow simulation and the actual scramjet experiments of Kay et al.<sup>4</sup> affirm the relevance to scramjet applications of the trends reported here, i.e., the decreased jet penetration with increasing amount of superheat, and the observed structural features and vaporization characteristics.

### Summary and Conclusions

The structure and penetration characteristics of transverse nitrogen jets injected at supercritical pressure into supersonic flow were examined experimentally and compared with those of subcooled ethanol jets. Shadowgraph images revealed the presence of large-scale structures for the case of supercritical nitrogen injection which were visible up to a normalized downstream distance of  $x/d_e \approx 55$ . The shadowgraph images also suggest that regions of unmixed primary stream gas penetrate well into the profile of the transverse fluid jet. Similar structural features do not appear to characterize subcooled ethanol jets injected at similar pressures.

The supercritical nitrogen jets penetrate less into a supersonic stream at a given downstream location than jets consisting of subcooled liquid ethanol injected at similar pressure. The current jet penetration results are in agreement with previous studies for subcritical nitrogen injection at comparable superheat, i.e., comparable values of the fluid vapor pressure/gas stream static pressure ratio. The jet penetration further decreases with increases in the degree of superheat. The ethanol penetration results are in agreement with the unheated water and acetone injection results of previous investigations.

Consideration of injection and supersonic flow conditions of previous investigations reveals that, in some cases, the vapor pressures of the injectants may have continually decreased with downstream distance as the injectant fluid was cooled by the cold supersonic stream, thus retarding the transition to vapor and enhancing jet penetration. This suggests that experiments to simulate scramjet flowfields must consider both the degree of superheat as well as the temperature difference between the injectant fluid and supersonic gas stream. Although resulting in a lower penetration than for nonvolatile, subcooled liquid injected at similar pressure, the supercritical fluid naturally results in a much more rapid transition from fluid to vapor than does the subcooled liquid. More rapid vaporization is unfortunately accompanied by poorer penetration, suggesting the existence of an optimum selection of

injection parameters in the tradeoff between penetration and vaporization.

### Acknowledgments

The authors acknowledge the financial support of United Technologies Corporation and the Air Force Office of Scientific Research AFRAPT Program, and helpful discussions with R. N. Guile, and the expert technical assistance of J. S. Wegge, R. W. Siegmund, and R. J. Haas.

### References

- Billig, F. S., "Research on Supersonic Combustion," AIAA Paper 92-0001, Jan. 1992.
- Nörtham, G. B., and Anderson, G. Y., "Supersonic Combustion Ramjet Research at Langley," AIAA Paper 86-0159, Jan. 1986.
- Waltrup, P. J., "Liquid Fueled Supersonic Combustion Ramjets: A Research Perspective of the Past, Present and Future," AIAA Paper 86-0158, Jan. 1986.
- Kay, I. W., Peschke, W. T., and Guile, R. N., "Hydrocarbon-Fueled Scramjet Combustor Investigation," *Journal of Propulsion and Power*, Vol. 8, No. 2, 1992, pp. 507-512.
- Schetz, J. A., Hawkins, P. F., and Lehman, H., "Structure of Highly Underexpanded Transverse Jets in a Supersonic Stream," *AIAA Journal*, Vol. 5, No. 5, 1966, pp. 882-884.
- Zukoski, E. E., and Spaid, F. W., "Secondary Injection of Gases into a Supersonic Flow," *AIAA Journal*, Vol. 2, No. 10, 1964, pp. 1689-1696.
- Orth, R. C., Schetz, J. A., and Billig, F. S., "The Interaction and Penetration of Gaseous Jets in Supersonic Flow," NASA CR-1386, July 1969.
- Hermanson, J. C., and Winter, M., "Mie Scattering Imaging of a Transverse, Sonic Jet in Supersonic Flow," *AIAA Journal*, Vol. 31, No. 1, 1993, pp. 129-132.
- Papamoschou, D., Hubbard, D. G., and Lin, M., "Observations of Supersonic Transverse Jets," AIAA Paper 91-1723, June 1991.
- Povinelli, F. P., Povinelli, L. A., and Hersch, M., "Supersonic Jet Penetration (up to Mach 4) into a Mach 2 Airstream," AIAA Paper 70-92, Jan. 1970.
- Cohen, L. S., Coulter, L. J., and Egan, W. J., "Penetration and Mixing of Multiple Gas Jets Subjected to a Cross Flow," *AIAA Journal*, Vol. 9, No. 4, 1971, pp. 718-724.
- Schetz, J. A., and Nejad, A. S., "The Effects of Viscosity and Surface Tension of Liquid Injectants on the Structural Characteristics of the Plume in a Supersonic Airstream," AIAA Paper 82-0253, Jan. 1982.
- Kush, E. M., and Schetz, J. A., "Liquid Jet Injection into a Supersonic Flow," AIAA Paper 72-1180, Dec. 1972; also *AIAA Journal*, Vol. 11, No. 9, 1973, p. 1223.
- Joshi, P. B., and Schetz, J. A., "Effect of Injector Shape on Penetration and Spread of Liquid Jets," *AIAA Journal*, Vol. 13, No. 9, 1975, pp. 1137-1138.
- Lienhard, J. H., and Stephenson, J. M., "Temperature and Scale Effects Upon Cavitation and Flashing in Free and Submerged Jets," *Journal of Basic Engineering*, Vol. 84, June 1966, pp. 525-532.
- Lienhard, J. H., and Day, J. B., "The Breakup of Superheated Liquid Jets," *Journal of Basic Engineering*, Vol. 88, Sept. 1970, pp. 515-522.
- Wu, K. J., Steinberger, R. L., and Bracco, F. V., "On the Mech-

anisms of Breakup of Highly Superheated Liquid Jets," *Combustion Inst. Central States Section/Combustion Inst.* 81-17, Warren, MI, March 1981.

<sup>18</sup>Solomon, A. S. P., Rupprecht, S. D., Chen, L. D., and Faeth, G. M., "Flow and Atomization in Flashing Injectors," *Atomisation and Spray Technology*, Vol. 1, No. 1, 1985, pp. 53-76.

<sup>19</sup>Kim, Y. K., Iwai, N., Suto, H., and Tsuruga, T., "Improvement of Alcohol Engine Performance by Flash Boiling Injection," *Society of Automotive Engineers of Japan (JSAE) Review* 2, April 1980, pp. 81-86.

<sup>20</sup>Newton, J. F., Jr., and Dowdy, M. W., "Investigation of Liquid and Gaseous Secondary Injection Phenomena on a Flat Plate with  $M = 2.01$  to  $M = 4.54$ ," *Jet Propulsion Lab.*, TR 32-542, Pasadena, CA, 1963.

<sup>21</sup>Kolpin, M. A., Horn, K. P., and Reichenbach, R. E., "Study of Penetration of a Liquid Injectant into a Supersonic Flow," *AIAA Journal*, Vol. 6, No. 5, 1968, pp. 853-858.

<sup>22</sup>Reichenbach, R. E., and Horn, K. P., "Investigation of Injectant Properties on Jet Penetration in a Supersonic Stream," *AIAA Journal*, Vol. 9, No. 3, 1971, pp. 469-472.

<sup>23</sup>Schetz, J. A., Hewitt, P. W., and Situ, M., "Transverse Jet Breakup and Atomization with Rapid Vaporization Along the Trajectory," *AIAA Journal*, Vol. 23, No. 4, 1985, pp. 596-603.

<sup>24</sup>Smith, D. R., Poggie, J., Konrad, W., and Smits, A. J., "Visualization of the Structure of Shock Wave-Turbulent Boundary Layer Interactions Using Rayleigh Scattering," *AIAA Paper* 91-0651, Jan. 1991.

<sup>25</sup>Landau, L. D., and Lifshitz, E. M., *Fluid Mechanics*, Pergamon Press, Oxford, England, UK, 1978.

Recommended Reading from Progress in Astronautics and Aeronautics

## High-Speed Flight Propulsion Systems

S.N.B. Murthy and E.T. Curran, editors

This new text provides a cohesive treatment of the complex issues in high speed propulsion as well as introductions to the current capabilities for addressing several fundamental aspects of high-speed vehicle propulsion development. Nine chapters cover Energy Analysis of High-Speed Flight Systems; Turbulent Mixing in Supersonic Combustion Systems; Facility Requirements for Hypersonic Propulsion System Testing; and more. Includes more than 380 references, 290 figures and tables, and 185 equations.

1991, 537 pp, illus, Hardback

ISBN 1-56347-011-X

AIAA Members \$54.95

Nonmembers \$86.95

Order #: V-137 (830)

Place your order today! Call 1-800/682-AIAA



American Institute of Aeronautics and Astronautics

Publications Customer Service, 9 Jay Gould Ct., P.O. Box 753, Waldorf, MD 20604  
FAX 301/843-0159 Phone 1-800/682-2422 9 a.m. - 5 p.m. Eastern

Sales Tax: CA residents, 8.25%; DC, 6%. For shipping and handling add \$4.75 for 1-4 books (call for rates for higher quantities). Orders under \$100.00 must be prepaid. Foreign orders must be prepaid and include a \$20.00 postal surcharge. Please allow 4 weeks for delivery. Prices are subject to change without notice. Returns will be accepted within 30 days. Non-U.S. residents are responsible for payment of any taxes required by their government.